Brain Research 1796 (2022) 148082

Contents lists available at ScienceDirect

Brain Research

journal homepage: www.elsevier.com/locate/brainres

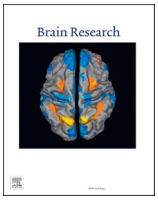

Influence of age and cognitive performance on resting-state functional connectivity of dopaminergic and noradrenergic centers

Michal Rafal Zareba [a,b,1], Wiktoria Furman [a,b,1,*], Marek Binder [b]

[a] Institute of Zoology and Biomedical Research, Faculty of Biology, Jagiellonian University, Krakow, Poland
[b] Institute of Psychology, Faculty of Philosophy, Jagiellonian University, Krakow, Poland

ARTICLE INFO

Keywords:
Ventral tegmental area
Substantia nigra
Locus coeruleus
Aging
Regional homogeneity
Visuomotor search

ABSTRACT

Aging is associated with structural and functional changes in the brain, with a decline in cognitive functions observed as its inevitable concomitant. The body of literature suggests dopamine and noradrenaline as prominent candidate neuromodulators to mediate these effects; however, knowledge regarding the underlying mechanisms is scarce. To fill this gap, we compared resting-state functional connectivity (FC) patterns of ventral tegmental area (VTA), substantia nigra pars compacta (SNc) and locus coeruleus (LC) in healthy young (20–35 years; N = 37) and older adults (55–80 years; N = 27). Additionally, we sought FC patterns of these structures associated with performance in tasks probing executive, attentional and reward functioning, and we compared the functional coupling of the bilateral SNc. The results showed that individual SNc had stronger coupling with ipsilateral cortical and subcortical areas along with the contralateral cerebellum in the whole sample, and that the strength of connections of this structure with angular gyrus and lateral orbitofrontal cortex predicted visuomotor search abilities. In turn, older age was associated with greater local synchronization within VTA, its lower FC with caudate, mediodorsal thalamus, and SNc, as well as higher FC of both midbrain dopaminergic seeds with red nuclei. LC functional coupling showed no differences between the groups and was not associated with any of the behavioral functions. To the best of our knowledge, this work is the first to report the age-related effects on VTA local synchronization and its connectivity with key recipients of dopaminergic innervation, such as striatum and mediodorsal thalamus.

1. Introduction

The process of aging is inevitably associated with substantial changes in the structure and functioning of the human brain (Tsvetanov et al., 2021). A prominent decline in cognitive functions such as attention, executive functioning, working memory, conceptual reasoning and visuospatial processing is commonly observed (Harada et al., 2013; Hedden and Gabrieli, 2004). Interestingly, certain other processes, such as reward responsiveness, are distinctly affected by aging depending on the context (e.g., type of reward), with older adults exhibiting diminished responsiveness to financial incentives (Dhingra et al., 2020) but greater sensitivity to social reward (Rademacher et al., 2014).

In the last two decades, there has been a prominent increase in the number of studies on aging in which resting-state functional magnetic resonance imaging (fMRI) was used as a primary method. The most consistent findings across different studies are a decline in functional connectivity within networks and an increase in functional connectivity between networks (Jockwitz and Caspers, 2021). However, little is known about the connection between age and alterations in the functional connectivity of neuromodulatory systems.

Dopamine and noradrenaline are two prominent candidate molecules for mediating the outlined effects of aging on brain functioning. Dopamine is mainly synthesized by neurons located in two adjacent midbrain structures: the ventral tegmental area (VTA) and the

Abbreviations: ACC, anterior cingulate cortex; BOLD, blood-oxygen-level-dependent; BAS, Behavioral Approach System; CSF, cerebrospinal fluid; DLPFC, dorsolateral prefrontal cortex; FC, functional connectivity; FDR, false discovery rate; FWE, family-wise error; fMRI, functional magnetic resonance imaging; LC, locus coeruleus; MRI, magnetic resonance imaging; ReHo, regional homogeneity; ROI, region of interest; SNc, substantia nigra pars compacta; TAP, Test of Attentional Performance; tSNR, temporal signal-to-noise ratio; TMT, Trail Making Test; VTA, ventral tegmental area; WM, white matter.

* Corresponding author at: Institute of Zoology and Biomedical Research, Faculty of Biology, Jagiellonian University, Krakow, Poland.
E-mail address: wiktoria.furman23@gmail.com (W. Furman).

[1] These authors contributed equally to this work.

https://doi.org/10.1016/j.brainres.2022.148082
Received 26 March 2022; Received in revised form 24 August 2022; Accepted 7 September 2022
Available online 14 September 2022

substantia nigra pars compacta (SNc; Bissonette and Roesch, 2016). The locus coeruleus (LC), located in the upper dorsolateral part of the brainstem, constitutes the primary source of noradrenaline in the brain (Szabadi, 2013).

Both dopaminergic and noradrenergic systems cover widespread connections throughout the brain and are strongly associated with multiple cognitive functions, such as reward processing, sustained attention, working memory, executive control and visuomotor search (Bäckman and Nyberg, 2013; Bellgrove et al., 2005; Berridge and Kringelbach, 2015; Chen et al., 2020; Ramos and Arnsten, 2007; Saloner et al., 2020; Schultz, 2016). In the course of aging, a reduction in the number of dopamine receptors and transporters is observed (Karrer et al., 2017). In turn, the locus coeruleus-noradrenergic system seems to be especially sensitive to degenerative changes related to aging, as a loss of LC neurons, along with overall noradrenergic disruption, is observed in the early stages of both Alzheimer's and Parkinson's diseases (for a review see: Peterson and Li, 2018). These findings suggest that differences in the functioning of both systems are likely to mediate the effects of age on different aspects of cognition.

To our knowledge, only three studies have been published so far regarding age-related distinctions in the connectivity of the main dopaminergic regions. In individuals ranging from 18 to 49 years old, older age was related to stronger coupling between VTA/SNc and the lateral prefrontal cortex, the superior temporal and parahippocampal gyri, as well as the cerebellum (Manza et al., 2015; Peterson et al., 2017; Zhang et al., 2016). Unlike VTA, SNc was also found to have greater connectivity with the angular gyrus (Peterson et al., 2017). The only negative association with age was reported for the coupling between VTA/SNc and the somatomotor cortex (Manza et al., 2015; Peterson et al., 2017; Zhang et al., 2016).

Zhang and colleagues were the first to examine the effects of aging on LC connectivity patterns (Zhang et al., 2016). They found that age was positively correlated with the strength of connections of the LC to the angular gyrus, the middle frontal gyrus, and the cerebellum; also, it was negatively correlated with connectivity to the parahippocampus and precuneus. Jacobs and others revealed a positive association between the connectivity of the left LC to the left parahippocampal gyrus and memory performance among healthy older subjects (Jacobs et al., 2015). Meanwhile, the connectivity between these structures was reduced in patients with amnestic mild cognitive impairment (Jacobs et al., 2015). Two other studies revealed nonlinear relationships between age and LC connectivity. Curvilinear associations between age and the functional connectivity of the left LC to the bilateral frontal, temporal and parietal cortical areas, as well as to the left nucleus basalis of Meynert were observed by Jacobs and colleagues (Jacobs et al., 2018). Recently, Song, Neal and Lee found a positive quadratic relationship between age and LC connectivity with sensory regions and a negative quadratic association between age and LC connectivity with frontal regions (Song et al., 2021).

In this study, we focused on dopaminergic and noradrenergic systems considering their important role in cognitive functioning and the evidence for substantial changes in these systems in the course of aging. With the usage of open-access data, we aimed to investigate whether aging affects the functional connectivity of dopaminergic and noradrenergic systems' targets over the whole brain. This work extends the previous findings by comparing the resting-state connectivity patterns of VTA, SNc and LC between young (aged 20–35) and older adults (aged 55–80), i.e., beyond the age range used in the papers published so far. Secondly, this study aimed to investigate the relationship between behavioral indices of cognitive and motivational processing and the functional connectivity patterns of the primary noradrenergic and dopaminergic nuclei. To the best of our knowledge, no previous works have attempted to find such associations for sustained attention, working memory, visuomotor search and set shifting. Additionally, this is the first study to investigate age-related differences in regional homogeneity (ReHo) within the dopaminergic midbrain. We expected the older group to have lower resting-state functional connectivity of the noradrenergic and dopaminergic seeds with a majority of cortical and subcortical regions; however, we did not exclude the possibility of finding regions with stronger coupling with both systems in the elderly, as these have been reported before.

2. Results

2.1. Whole-brain functional connectivity of VTA, SNc and LC

All dopaminergic regions of interest (ROIs) – VTA and SNc – displayed extensive positive connectivity to a number of cortical and subcortical targets, thus reflecting their widespread anatomical connections. The targets included the bilateral cingulate, the dorsomedial prefrontal and the lateral orbitofrontal cortex, the inferior frontal gyrus pars opercularis, the parieto-occipital sulcus, the medial temporal cortices, the insula, the caudate nucleus, the putamen, the nucleus accumbens and the globus pallidus, the thalamus, the pons, the midbrain and the cerebellum. Furthermore, they shared negative connectivity to the bilateral motor and somatosensory cortices, as well as parts of the superior and inferior parietal lobes. All seeds were also negatively coupled to the visual areas, with the positive coupling between the right SNc and the bilateral primary visual cortex being the only exception.

Both left and right LC showed positive connectivity to the bilateral anterior cingulate cortex (ACC), the thalamus, the cerebellum and the brainstem, and negative connectivity to the bilateral primary motor and somatosensory cortices, the precuneus, the superior parietal lobules, as well as the right inferior parietal lobule and the right superior frontal gyrus. The right but not the left LC was positively coupled with the bilateral hippocampus and negatively coupled with the left superior frontal gyrus. The left LC was negatively connected to the bilateral visual cortices, whereas in the right LC the relationship was present only for the ipsilateral regions. The connectivity patterns are depicted in Supplementary Figs. 1–5.

The comparison of the temporal signal-to-noise ratio (tSNR) between the bilateral ROIs showed higher values of this metric for the right LC versus the left LC (false discovery rate; FDR = 0.005) and no distinction between both SNc regions (FDR = 0.934; see Supplementary Table 1 for more details). As a result, individual tSNRs were included in the model contrasting the connectivity of the left and right LC. Despite the observed differences in the one-sample t-tests' results, a direct comparison of the connectivity strength between the left and right LC yielded no significant results. In turn, contrasting the coupling patterns of the left and right SNc revealed that each seed showed greater coupling with the cerebral cortex and midbrain regions located ipsilaterally to the given ROI. The opposite connectivity pattern was observed for the cerebellum as the left SNc was more strongly connected to the right cerebellar hemisphere. The results are presented in more detail in Supplementary Fig. 6 and Supplementary Table 2.

2.2. The impact of age on connectivity patterns

The younger group was found to have higher tSNR in the left LC (FDR = 0.008), right LC (FDR = 0.007), left SNc (FDR = 0.007) and right SNc (FDR = 0.034) compared to the older group. As a consequence, individual tSNRs were included as covariate in the between-group comparisons for these ROIs. By contrast, tSNR in VTA did not differ between the younger and older subjects (FDR = 0.189; more details in Supplementary Table 1).

No effect of age on the connectivity of the left or right LC was found. In turn, several differences were observed for the dopaminergic seeds. The older group had lower VTA functional connectivity with the bilateral caudate nuclei and the mediodorsal thalamus. Older age was further associated with greater signal correlation between the left SNc and the ipsilateral dorsolateral prefrontal cortex (DLPFC). Additionally, the

patterns of VTA and SNc connectivity to other midbrain structures also differed between age groups. In older adults, VTA had higher resting-state connectivity to the bilateral red nucleus, while the right SNc was more strongly connected to the midbrain area adjacent to the unilateral red nucleus. At the same time, bilateral SNc seeds showed a lower extent of connectivity to VTA and neighboring voxels. The results are shown in Table 1 and Fig. 1.

2.3. Age-related differences in regional homogeneity of the dopaminergic seeds

The younger group was found to have higher tSNR in the SVC mask of the dopaminergic regions (FDR = 0.022; see Supplementary Table 1 for more details), and subsequently tSNR was accounted for in the ReHo model. The analysis revealed that the older group had greater ReHo within VTA. Suprathreshold statistics were found for a cluster consisting of 13 of the 105 voxels in the SVC mask (MNI: x = 8, y = -13, z = -12; peak voxel *T*-stat = 3.97; see Fig. 2).

2.4. Age-related differences in behavioral measures

The older group was characterized by lower sustained attention (longer reaction times in Test of Attentional Performance (TAP) (Alertness; FDR = 0.002), lower visuomotor search capability (longer completion time of Trail Making Test (TMT) Part A; FDR < 0.001) and lower set shifting (greater difference between TMT-B and TMT-A completion times; FDR < 0.001). Interestingly, while the older participants performed worse in the TAP Working Memory task (i.e., fewer correct responses; FDR = 0.020), the reaction times of the successful trials did not differ significantly between the groups (FDR = 0.081). Additionally, the older and younger subjects scored similarly in Behavioral Approach System (BAS) Reward Responsiveness (FDR = 0.306). The results are described in more detail in the Supplementary Table 3.

2.5. Functional connectivity associated with behavioral results

A single significant correlation between the tSNR and cognitive outcomes was found for the left SNc and the reaction times in the TAP Alertness task, which measures sustained attention (FDR = 0.014; ρ = -0.37; more details in Supplementary Fig. 7 and Supplementary Table 4). Thus, the model investigating the connectivity patterns of the region related to task performance included tSNR as an additional covariate.

The only associations between resting-state functional connectivity and behavioral measures were found for the right SNc and the TMT-A visuomotor task. The connectivity strength of the right SNc with both the left angular gyrus (R = 0.67) and the right lateral orbitofrontal cortex (R = 0.64) was positively correlated with the completion time of the task, i.e., the greater the coupling, the worse the performance. The results are shown in more detail in Table 2 and Fig. 3. The scatterplots depicting the relationship of the TMT-A completion time with connectivity strength between the brain areas are presented in Supplementary Figs. 8 and 9.

Table 1
Age-related differences in resting-state functional connectivity of dopaminergic nuclei (voxel-level FDR < 0.05 and cluster extent of minimum 10 voxels).

MNI	Location	Voxels	Directionality	*T*-stat
VTA				
5, −15, 10	B red nucleus	31	Old > Young	6.72
8, 12, 8	R caudate nucleus	16	Young > Old	5.82
−9, 12, 11	L caudate nucleus	15	Young > Old	5.58
1, −20, 6	B mediodorsal thalamus	10	Young > Old	5.32
L SNc				
–22, 19, 47	L dorsolateral prefrontal cortex	13	Old > Young	5.13
−4, −15, −17	B ventral tegmental area	10	Young > Old	6.05
R SNc				
10, −15, −8	R midbrain	13	Old > Young	5.45
8, −17, −17	B ventral tegmental area	12	Young > Old	5.69

3. Discussion

3.1. Functional connectivity patterns of VTA, SNc and LC

The dopaminergic connectivity patterns in our study considerably overlap with those reported in earlier studies (Manza et al., 2015; Peterson et al., 2017; Zhang et al., 2016). The obtained pattern of resting-state functional connectivity of the LC is also consistent with previous works (Liebe et al., 2020; Zhang et al., 2016). To the best of our knowledge, this is the first study to show differences in the functional connectivity between the left and right SNc. The observed coupling pattern, i.e., greater connectivity with the ipsilateral subcortical and cortical regions along with stronger correlation with the contralateral cerebellum, is in line with the results of anatomical studies on rodents, primates and humans (Meola et al., 2016; Molochnikov and Cohen, 2014). Considering the strong laterality of symptoms at the onset of Parkinson's disease, treating the right and left SNc as separate seed regions could hold some potential in clinical MRI applications (Heinrichs-Graham et al., 2017).

3.2. Age-related differences in dopaminergic connectivity

Our study is the first to show that older age is linked to lower VTA functional connectivity with the caudate nucleus and the mediodorsal thalamus, two key telencephalic recipients of dopaminergic innervation. These results correspond well with an age-related loss of dopamine transporters and receptors in the former area (Karrer et al., 2017). Additionally, the finding of greater coupling of the left SNc with the left DLPFC in older adults adds to an earlier report that showed a positive correlation between the coupling of the VTA/SNc with the lateral prefrontal cortex and age in a sample aged 18–49 years (Manza et al., 2015).

The caudate and the mediodorsal thalamus, where we observed lower functional connectivity with VTA in older adults, are both important hubs for integrating information from multiple neural systems, including emotional, cognitive, sensory and motor circuits (Haber, 2014; Mitchell and Chakraborty, 2013). Due to these neural connections, the alterations in functional connectivity with these structures may constitute a correlate of behavioral deterioration in more than one specific domain. For example, the lower connectivity of dopaminergic areas to the caudate nucleus could be related to the psychomotor slowing of older individuals (Karim et al., 2020). This mechanism could coexist with the observed greater coupling of VTA/SNc to the red nucleus, which is known to exert a modulatory effect on cortico-striatal networks and has been implicated in motor functions (Bostan and Strick, 2018; Meola et al., 2016). All in all, these two findings complement previous aging studies which reported differences in VTA/SNc connectivity with the somatomotor cortex and the cerebellum, further suggesting the link between dopaminergic dysfunction and motor deterioration in older adults (Manza et al., 2015; Peterson et al., 2017). In turn, greater correlation between the left SNc and the DLPFC may demonstrate involvement of this circuit in age-related differences in top-down modulation of appropriate behavioral responses (Glasser et al., 2016).

Our analyses also revealed age-related differences in the functional organization within the dopaminergic midbrain. In older adults, bilateral SNc seeds were less strongly coupled with the VTA. Additionally, the same group was characterized by greater ReHo in the VTA. Overall, our study is the first to indicate that aging is associated with differences in connectivity between dopaminergic areas, as well as local

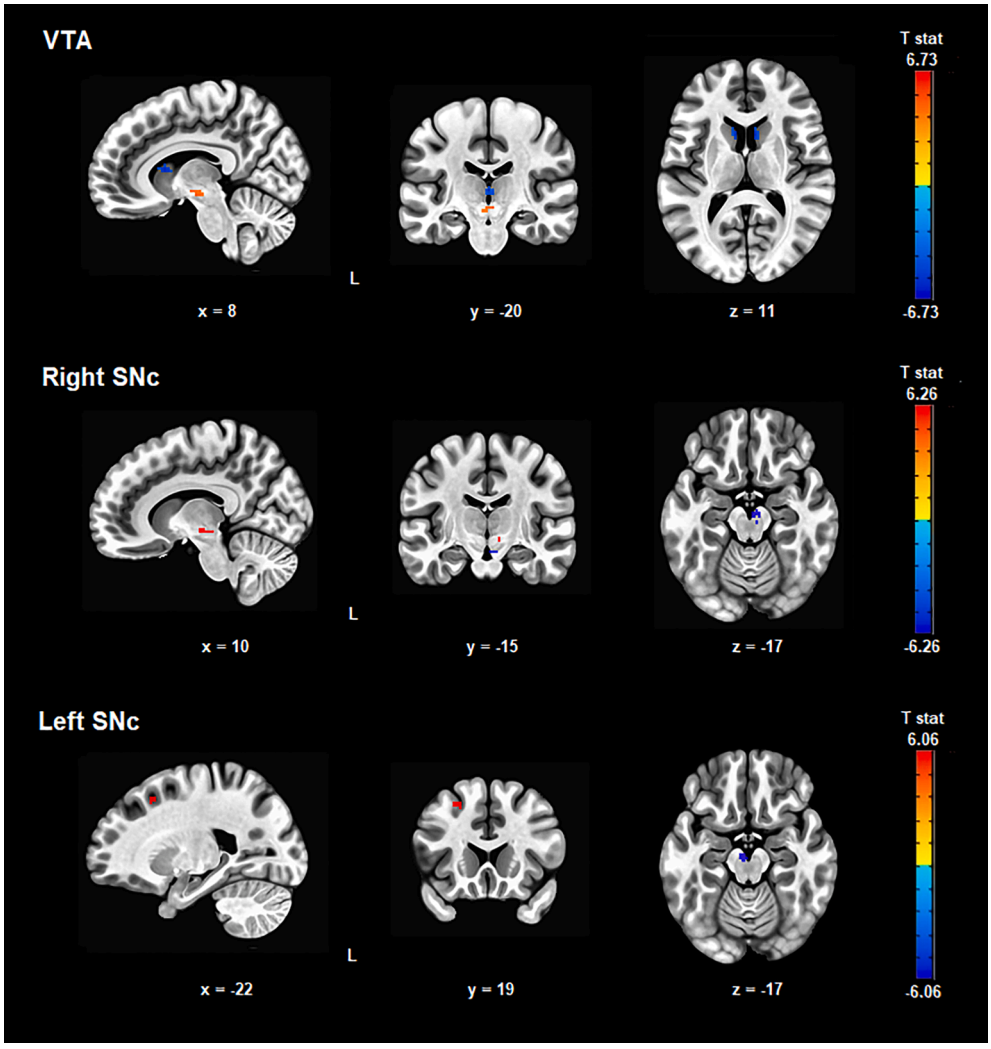

Fig. 1. Areas of greater (warm colors) and lower (cold colors) resting-state functional connectivity with VTA and SNc in the elderly group.

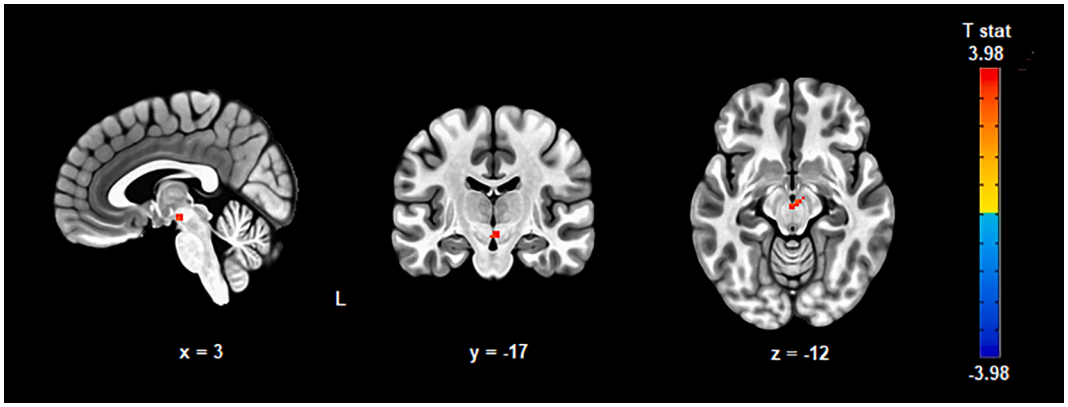

Fig. 2. The elderly group was found to have greater regional homogeneity (ReHo) within VTA.

synchronization within them. The lower functional connectivity between the SNc and the VTA is in line with weaker coupling within resting-state functional systems in older adults (Jockwitz and Caspers, 2021). The local synchronization, measured with ReHo, has been shown to vary across the brain, with lower values being characteristic of areas with more complex functions (Song et al., 2014). As the VTA is known to be less vulnerable to age-related pathological degeneration than the SNc (Fu et al., 2016), which is supported by our tSNR group comparisons, these results might be a marker of the differential aging trajectories and diminished communication between these two dopaminergic regions.

3.3. *Aging affects several cognitive domains but not reward responsiveness*

In line with the previously published research, we found that older

Table 2
Resting-state functional connectivity patterns of dopaminergic seeds correlated with behavioral performance (voxel-level FDR < 0.05 and cluster extent of minimum 10 voxels).

Seed	MNI	Location	Voxels	Pearson's correlation [r]	F-stat
TMT-A					
R SNc	−36, −61, 36	L angular gyrus	27	0.67	28.28
R SNc	37, 42, −15	R orbitofrontal cortex	14	0.64	37.69

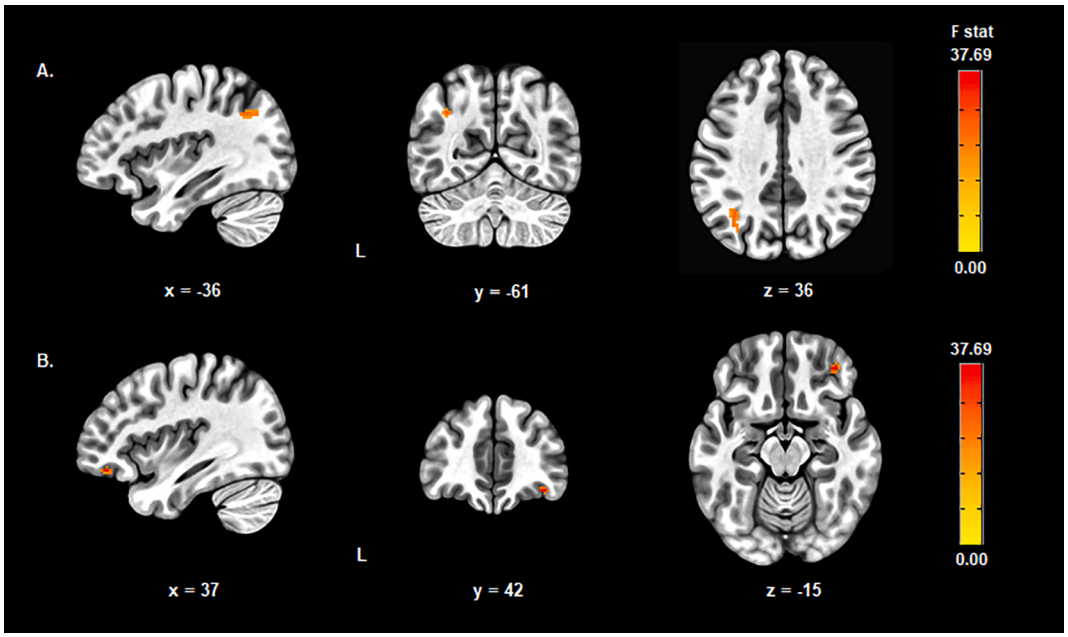

Fig. 3. The functional connectivity of the right SNc with (A) the left angular gyrus and (B) the right lateral orbitofrontal cortex was found to be positively correlated with the completion time of the TMT-A task probing visuomotor search capabilities.

adults performed worse in the following domains: sustained attention (Vallesi et al., 2021), visuomotor search and executive control functions (Hu et al., 2018; St-Hilaire et al., 2018), as well as working memory accuracy (Bopp and Verhaeghen, 2020). Surprisingly, the group difference in the mean correct response time in the working memory task only approached the significance level (FDR = 0.081), which might be related to the limited sample size of our work, especially as a recently published *meta*-analysis investigating the effects of age on the performance in the 2-back task, which is analogous to the TAP Working Memory task, showed a significant negative effect of age on both accuracy and overall mean response times (Bopp and Verhaeghen, 2020). Last but not least, similar levels of reward responsiveness in the two groups are also in line with a vast body of research showing that value encoding of rewarding outcomes is largely intact in elderly individuals (Swirsky and Spaniol, 2019).

3.4. tSNR and functional connectivity of the SNc is linked to cognitive functions

Our investigation revealed a moderate negative correlation (ρ = -0.37) between the tSNR of the left SNc and mean reaction times in the sustained attention task. To the best of our knowledge, this is the first report showing an association between tSNR of dopaminergic regions and cognitive abilities. Our analyses further revealed that the connectivity strength of the right SNc with both the left angular gyrus and the right lateral orbitofrontal cortex was positively correlated with the completion time of the TMT-A task, i.e., the greater the coupling, the worse the visuomotor performance. The effect sizes of these two associations (R = 0.64–0.67) should, however, be treated with caution as circular analyses are known to greatly overestimate the true effect strengths (Kriegeskorte et al., 2010). According to the Neurosynth database, the location of the angular gyrus cluster maps onto the edge of the medial frontoparietal (default mode) network, which is expected not to have a positive correlation with areas involved in visuomotor search (Yarkoni et al., 2011). The lateral orbitofrontal cortex, where the other cluster was found, is known to be involved in movement inhibition (Aron and Poldrack, 2006). As elevated dopaminergic transmission promotes movement (Minassian et al., 2016), the negative association between task performance and the connectivity of the right SNc with the right lateral orbitofrontal cortex may indicate that anti-correlation between these two structures is related to appropriate motor behavior selection. Interestingly, the part of the lateral orbitofrontal cortex associated with the performance in the task was different from the one identified as having positive coupling with the right SNc in the one-sample *t*-test. This could indicate the existence of subdivisions within the lateral orbitofrontal cortex that are differentially associated with dopaminergic transmission.

Despite finding age-related VTA/SNc connectivity differences in several structures implicated in the studied behavioral paradigms, none of these were replicated in association with the task performance, which might be related to insufficient sample size and whole-brain calculations (Adrián-Ventura et al., 2019).

3.5. Limitations and future directions

The number of subjects is the major limitation of this study and a probable reason for not finding any significant age- and behavior-related findings for LC connectivity and the consequent failure to reproduce earlier aging reports. A larger sample size would have increased the statistical power of the analyses, making them better suited to detect

more subtle differences in connectivity patterns. Furthermore, knowing the precise age of participants and having a continuous age distribution would have enabled the investigation of the linear relationship between age and resting-state connectivity. On the other hand, the data acquisition parameters used in this study and the relative demographic homogeneity of both studied groups, compared to other available datasets, allowed more precise imaging of the processes of interest, which speaks in favor of the results' reliability. Future longitudinal studies are warranted to confirm the cross-sectional age-related differences in the connectivity of the VTA and the SNc that are reported in this study. Additionally, taking into account the distinct structural connectivity patterns of SNc subdivisions (Zhang et al., 2017), it would be beneficial to study whether their tractography differences are indeed reflected in resting-state connectivity and the behavioral measures these coupling patterns are correlated with. Preferably, the delineation of ROIs should be achieved in a data-driven manner, for example by using neuromelanin-sensitive imaging, as this would better account for interindividual variability. Furthermore, knowing the role of LC in regional blood flow control, it would be highly beneficial for future studies to account for cardiac measures in the analyses, which was not possible in the case of the current study.

4. Conclusions

Our findings show weaker long range VTA connectivity with the caudate and the mediodorsal thalamus, together with greater coupling of the SNc with the DLPFC in the elderly. Additionally, age is related to altered local connectivity within dopaminergic regions observed as greater VTA ReHo and weaker VTA-SNc coupling in the older group. Furthermore, this study links the functional characteristics of the SNc with visuomotor skills and sustained attention; it also underlines the connectivity differences between bilateral SNc. In conclusion, our study shows that age is associated with differences in local connectivity within dopaminergic centers, and their coupling with both cortical and subcortical brain regions serves integrative and executive functions.

5. Materials and methods

5.1. Dataset

The anonymized MRI and behavioral data were obtained from the Max Planck Institut Leipzig Mind-Brain-Body Dataset (Babayan et al., 2019). Out of the 227 subjects available in the database, only 134 met the initial inclusion criteria, i.e., right-handedness, secondary-level education, no psychiatric, neurological or substance abuse history, drug-free. The participants' age was provided only as a five-year bracket instead of specific values for stronger anonymity protection. Thus, the selected subjects were put into two age groups: 20–35 (N = 92) and 55–80 (N = 42). All participants from the elderly group matching the inclusion criteria were included in the sample. The size of the younger group was reduced to 42 subjects by the process of random selection to match the size of the elderly group. As a result of the fMRI data preprocessing, 5 subjects from the younger group and 15 participants from the elderly group were excluded from the analysis due to: excessive head motion (>fMRI voxel size. i.e., 2.3 mm; 4 younger and 10 elderly), significant brainstem signal loss resulting from susceptibility artifacts (1 younger and 2 elderly), and unsatisfactory brainstem alignment between anatomical and functional data (3 elderly). Thus, the final sample consisted of 37 younger (16 females) and 27 elderly (14 females) subjects. More motion-related dropouts in the older group are typical of fMRI experiments (Madan, 2018).

5.2. Behavioral data

The behavioral data chosen for the analyses were associated with several cognitive domains that are presumably affected by the dopamine and noradrenaline networks. Sustained attention was measured as a mean reaction time in the Alertness subtest of the TAP (Zimmermann and Fimm, 2012). Verbal working memory capacity was tested with the Working Memory subtest of TAP (Zimmermann and Fimm, 2012). The mean reaction times of the correct responses and the percentage of correct trials were chosen as variables of interest. The visuomotor capabilities (visual search) and executive functions (set shifting) were investigated using TMT Part A and Part B (Reitan and Wolfson, 2004). The completion time of TMT-A was treated as a measure of visuomotor search capability, while the difference between the completion times of TMT-B and TMT-A was taken into the analyses as the index of set shifting. Lastly, reward sensitivity was assessed with the Reward Responsiveness subscale of the BAS questionnaire (Carver and White, 1994), with the total score included in the behavioral models. The behavioral paradigms are described in more detail in Supplementary Data S1.

5.3. Behavioral data group-level analysis

The statistical analysis of behavioral data was performed in R (version 4.0.3; R Core Team, 2021). Separate models were created for each measure. They consisted of the behavioral score as the dependent variable, and the independent variables were age (factor) and sex (covariate). All subjects received the same level of education (i.e., secondary), thus it was not included in all the designs throughout the study. The parametric ANCOVA computations were performed with the use of anova function. When the data did not adhere to the assumptions of parametric analysis (i.e., non-normal distribution of the residuals), a non-parametric rank-based ANCOVA (raov function; Kloke and McKean, 2000) was utilized. The correction for multiple comparisons was achieved by using the FDR. Due to missing behavioral data, one subject (1 elderly female) was excluded from all the TMT-A and TMT-B analyses, and four participants (1 young female, 2 young males, and 1 elderly male) were not included in all the BAS Reward Responsiveness models.

5.4. MRI data acquisition and preprocessing

The MRI scanning sessions were performed on a 3 Tesla scanner (MAGNETOM Verio, Siemens Healthcare GmbH, Erlangen, Germany) equipped with a 32-channel head coil. High-resolution anatomical images were acquired using T1 MP2RAGE sequence (176 sagittal slices; 1 mm isotropic voxel size; TR = 5000 ms; TE = 2.92 ms; flip angle 1/flip angle 2 = 4°/5°; GRAPPA acceleration factor 3). The T2*-weighted resting-state fMRI data were collected with gradient echo planar multiband imaging sequence (64 axial slices acquired in interleaved order; 2.3 mm isotropic voxel size; TR = 1400 ms; TE = 30 ms; flip angle = 69°; multiband acceleration factor = 4). Participants were instructed to stay awake and lie still with their eyes open while looking at a low-contrast fixation cross. The functional data of each subject consisted of 657 volumes, resulting in a scan duration of 15 mins 30 s.

The anatomical data were preprocessed in the Computational Anatomy Toolbox (CAT12; Gaser and Dahnke, 2016). Each subject's T1-weighted image was skullstripped and segmented into gray matter, white matter (WM) and cerebrospinal fluid (CSF). The resulting brain image was used to coregister the functional data, whereas the WM and CSF segments were binarized and resampled to the fMRI resolution for the signal from these tissues to be extracted and used as regressors in the resting-state data denoising.

The functional data preprocessing stream was performed in FSL (fieldmap correction; Jenkinson et al., 2012) and AFNI (all other steps; Cox, 1996). The initial steps included: deleting the first five volumes (to allow for signal equilibration and steady state), despiking, slice-timing, motion (to the median volume) and fieldmap corrections. The resulting images were later coregistered to the skullstripped anatomical data. Subsequently, they were prewhitened, detrended, denoised (14 regressors: 6 original motion parameters; 6 motion parameters

derivatives; WM and CSF signal) and band-pass filtered in the 0.009–0.08 Hz range. The lack of inclusion of cardiac and respiratory parameters in the denoising procedure was guided by the fact that these measures were not available for all subjects included in the analyses, thus they were not used to ensure uniform preprocessing strategy across participants.

5.5. Seed regions and whole-brain functional connectivity

The seed regions for the resting-state functional connectivity analyses were derived from probabilistic atlases. Due to the small volume and proximity of the bilateral VTA, we decided to use a single ROI encompassing the structures on both sides of the brain, based on the work of Murty et al. (2014). In turn, the left and right SNc seeds were taken from the atlas created by Pauli and colleagues (Pauli et al., 2018), which delineated the substantia nigra (SN) subdivisions and thus enabled us to locate the signal of interest more precisely. The left and right LC ROIs were created on the basis of the mask created by Betts and colleagues (Betts et al., 2017).

To reduce the extent of mixing the signal between the VTA and bilateral SNc seeds through smoothing, as well as the potential effect of differences in ROI size on observed connectivity patterns, we thresholded the probabilistic ROIs. The arbitrarily chosen cut-off points were 0.97 for the VTA seed and 0.1 for the bilateral SNc seeds. No such thresholding was applied to the bilateral LC seeds. The resulting five ROIs were nonlinearly transformed from MNI space to each subject's brain image. Fig. 4 shows the location of the seeds in an example participant of our study. Across the cohort, the average ROI volume was 349.61 (±53.94) mm^3 for VTA, 278.89 (±45.28) mm^3 for the left SNc, 288.40 (±40.48) mm^3 for the right SNc, 89.95 (±28.21) mm^3 for the left LC, and 90.24 (±29.32) mm^3 for the right LC.

Before performing whole-brain seed-based functional connectivity calculations, the preprocessed resting-state volumes were spatially smoothed with a Gaussian kernel of 4 mm FWHM for the VTA and the bilateral SNc, and with a Gaussian filter of 3 mm FWHM for the bilateral LC. Subsequently, the seed time courses of the blood-oxygen-level-dependent (BOLD) signal were produced by averaging the BOLD time-series from all voxels in each seed. The correlations were computed between these mean time courses of every ROI and all other voxels in the brain. To normalize the data distribution, the Pearson correlation coefficients r were converted to z-scores using Fisher's z transform. The resulting maps were normalized to the MNI space to allow group-level analysis.

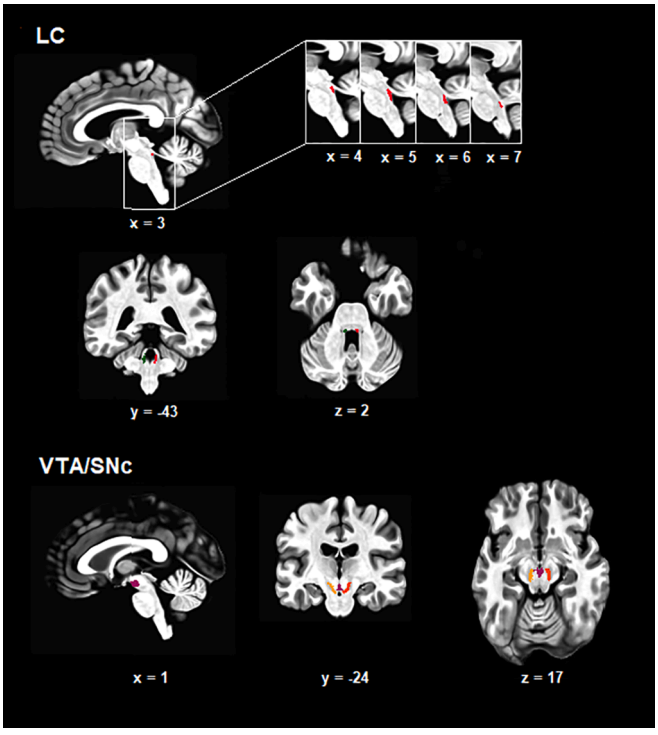

Fig. 4. Location of regions of interest (ROIs) in an example subject of the current study. The panel above shows the location of the left (dark green) and right (red) locus coeruleus (LC). The panel below shows the location of bilateral ventral tegmental area (VTA; purple), as well as the left (orange) and right (red) substantia nigra pars compacta (SNc).

5.6. Seed-based functional connectivity group-level analysis

All statistical analyses of the seed-based whole-brain functional connectivity data were performed using AFNI's 3dMVM program (Chen et al., 2014). The following comparisons were made: (i) one-sample t-tests of VTA, the left and right SNc, and the left and right LC functional connectivity; (ii) paired t-tests comparing the connectivity patterns of the bilateral SNc and LC in the whole sample; (iii) independent samples (old versus young) t-tests of each seed's whole-brain functional connectivity. The primary models consisted of age group as the factor, with sex as a covariate. Additionally, for each ROI we calculated the tSNR, defined as the mean signal in a ROI across its undenoised time course divided by the signal's standard deviation. Subsequently, we compared the tSNR in each ROI between the groups, as well as between the bilateral LC and the SNc in the entire sample. In the case of statistically significant differences, tSNR was included in the models as the second covariate.

To assess the resting-state functional connectivity patterns associated with behavioral results, we performed the multiple regression computations with resting-state functional connectivity maps as dependent variables, behavioral measures as the predictors, and sex as a confound, separately for each of the five behavioral domains (i.e., sustained attention, visuomotor search, set shifting, working memory and reward responsiveness) and each of the five seeds. As the cognitive scores were not normally distributed, we performed Spearman's correlations to investigate whether the tSNR of each ROI was significantly associated with any of the behavioral outcomes; in the case of significant findings, tSNR was included in the models as an additional covariate. Taking that the fMRI results were available in the form of F-statistics, which precludes assessing the direction of effects, mean Z values from the suprathreshold clusters were extracted and subsequently correlated with behavioral scores using R (version 4.0.3).

For the one-sample t-tests of seed-based functional connectivity, the correction for multiple comparisons was achieved through cluster-level family-wise error rate (FWE < 0.05) following voxel-level thresholding at $p < 0.001$ uncorrected. The cluster-forming thresholds were 152 voxels for LC and 192 voxels for the dopaminergic seeds. In the case of all other analyses, voxel-level FDR (<0.05) was applied. The respective FDR cluster-forming thresholds were: 40 voxels for the comparison of the connectivity patterns between the left and right SNc, and 10 voxels for all the remaining analyses The decision to use cluster-level FWE for one-sample t-tests of seed-based functional connectivity was guided by the fact that resting-state coupling patterns of VTA, SNc and LC have already been established in the literature, and this analysis served as a means of quality control for seed location. On the other hand, using voxel-level FDR correction in the remaining analyses was meant to increase their statistical power.

5.7. Regional homogeneity calculation and group-level analysis

To assess whether age was also associated with differences in the local resting-state functional connectivity within the dopaminergic regions, ReHo analysis was performed (Zang et al., 2004). ReHo measures the similarity of the time-courses of the neighboring voxels (7 in the case of our study) in a voxel-wise manner using Kendall's coefficient of

concordance. Due to the small volume of LC ROIs in our study, their oblong shape, and the relatively large distance between the left and right ROI, we decided to leave out the ReHo calculation for the noradrenergic seeds.

ReHo calculations were performed for the preprocessed resting-state data with the usage of AFNI's 3dReHo program. To standardize the scores of each participant, the ReHo value of each voxel was divided by the respective brain-wise mean ReHo. No spatial smoothing was applied. The resulting images were transformed into the MNI space to allow a group-level comparison. The statistical analysis was done with small volume correction (SVC; i.e., within a mask consisting solely of the dopaminergic seeds) using AFNI's 3dMVM program (Chen et al., 2014). The primary model consisted of age (factor) and sex (covariate). Similarly to the seed-based connectivity analyses, we calculated tSNR for the SVC mask and compared it between the groups. The decision whether or not to include it as an additional covariate in the model was based on the significance of the group comparison. The correction for multiple comparisons in the ReHo analysis was performed with voxel-level FDR (<0.05) and a cluster-forming threshold of 7 voxels.

Declaration of Competing Interest

The authors declare that they have no known competing financial interests or personal relationships that could have appeared to influence the work reported in this paper.

Data availability

This work was performed using a widely available open dataset (Babayan et al., 2019). https://www.nature.com/articles/sdata2018308.

Appendix A. Supplementary data

Supplementary data to this article can be found online at https://doi.org/10.1016/j.brainres.2022.148082.

References

Adrián-Ventura, J., Costumero, V., Parcet, M.A., Ávila, C., 2019. Reward network connectivity "at rest" is associated with reward sensitivity in healthy adults: A resting-state fMRI study. Cogn Affect Behav Neurosci. 19 (3), 726–736. https://doi.org/10.3758/s13415-019-00688-1.

Aron, A.R., Poldrack, R.A., 2006. Cortical and subcortical contributions to Stop signal response inhibition: role of the subthalamic nucleus. J Neurosci. 26 (9), 2424–2433. https://doi.org/10.1523/JNEUROSCI.4682-05.2006.

Babayan, A., Erbey, M., Kumral, D., Reinelt, J.D., Reiter, A.M.F., Röbbig, J., Schaare, H. L., Uhlig, M., Anwander, A., Bazin, P.L., Horstmann, A., Lampe, L., Nikulin, V.V., Okon-Singer, H., Preusser, S., Pampel, A., Rohr, C.S., Sacher, J., Thöne-Otto, A., Trapp, S., Nierhaus, T., Altmann, D., Arelin, K., Blöchl, M., Bongartz, E., Breig, P., Cesnaite, E., Chen, S., Cozatl, R., Czerwonatis, S., Dambrauskaite, G., Dreyer, M., Enders, J., Engelhardt, M., Fischer, M.M., Forschack, N., Golchert, J., Golz, L., Guran, C.A., Hedrich, S., Hentschel, N., Hoffmann, D.I., Huntenburg, J.M., Jost, R., Kosatschek, A., Kunzendorf, S., Lammers, H., Lauckner, M.E., Mahjoory, K., Kanaan, A.S., Mendes, N., Menger, R., Morino, E., Näthe, K., Neubauer, J., Noyan, H., Oligschläger, S., Panczyszyn-Trzewik, P., Poehlchen, D., Putzke, N., Roski, S., Schaller, M.C., Schieferbein, A., Schlaak, B., Schmidt, R., Gorgolewski, K. J., Schmidt, H.M., Schrimpf, A., Stasch, S., Voss, M., Wiedemann, A., Margulies, D.S., Gaebler, M., Villringer, A., 2019. A mind-brain-body dataset of MRI, EEG, cognition, emotion, and peripheral physiology in young and old adults. Sci Data. 6, 180308 https://doi.org/10.1038/sdata.2018.308.

Bäckman, L., Nyberg, L., 2013. Dopamine and training-related working-memory improvement. Neuroscience & Biobehavioral Reviews 37 (9), 2209–2219.

Bellgrove, M.A., Hawi, Z., Kirley, A., Gill, M., Robertson, I.H., 2005. Dissecting the attention deficit hyperactivity disorder (ADHD) phenotype: sustained attention, response variability and spatial attentional asymmetries in relation to dopamine transporter (DAT1) genotype. Neuropsychologia. 43 (13), 1847–1857. https://doi.org/10.1016/j.neuropsychologia.2005.03.011.

Berridge, K.C., Kringelbach, M.L., 2015. Pleasure systems in the brain. Neuron. 86 (3), 646–664. https://doi.org/10.1016/j.neuron.2015.02.018.

Betts, M.J., Cardenas-Blanco, A., Kanowski, M., Jessen, F., Düzel, E., 2017. In vivo MRI assessment of the human locus coeruleus along its rostrocaudal extent in young and older adults. Neuroimage. 163, 150–159. https://doi.org/10.1016/j.neuroimage.2017.09.042.

Bissonette, G.B., Roesch, M.R., 2016. Development and function of the midbrain dopamine system: what we know and what we need to. Genes Brain Behav. 15 (1), 62–73. https://doi.org/10.1111/gbb.12257.

Bopp, K.L., Verhaeghen, P., 2020. Aging and n-Back Performance: A Meta-Analysis. J Gerontol B Psychol Sci Soc Sci. 75 (2), 229–240. https://doi.org/10.1093/geronb/gby024.

Bostan, A.C., Strick, P.L., 2018. The basal ganglia and the cerebellum: nodes in an integrated network. Nat Rev Neurosci. 19 (6), 338–350. https://doi.org/10.1038/s41583-018-0002-7.

Carver, C.S., White, T.L., 1994. Behavioral inhibition, behavioral activation, and affective responses to impending reward and punishment: the BIS/BAS scales. J Pers Soc Psychol. 67 (2), 319. https://doi.org/10.1037/0022-3514.67.2.319.

Chen, G., Adleman, N.E., Saad, Z.S., Leibenluft, E., Cox, R.W., 2014. Applications of multivariate modeling to neuroimaging group analysis: a comprehensive alternative to univariate general linear model. Neuroimage. 99, 571–588. https://doi.org/10.1016/j.neuroimage.2014.06.027.

Chen, P.S., Jamil, A., Liu, L.C., Wei, S.Y., Tseng, H.H., Nitsche, M.A., Kuo, M.F., 2020. Nonlinear Effects of Dopamine D1 Receptor Activation on Visuomotor Coordination Task Performance. Cereb Cortex. 30 (10), 5346–5355. https://doi.org/10.1093/cercor/bhaa116.

Cox, R.W., 1996. AFNI: software for analysis and visualization of functional magnetic resonance neuroimages. Comput Biomed Res. 29 (3), 162–173. https://doi.org/10.1006/cbmr.1996.0014.

Dhingra, I., Zhang, S., Zhornitsky, S., Le, T.M., Wang, W., Chao, H.H., Levy, I., Li, C.R., 2020. The effects of age on reward magnitude processing in the monetary incentive delay task. Neuroimage. 207, 116368 https://doi.org/10.1016/j.neuroimage.2019.116368.

Fu, Y., Paxinos, G., Watson, C., Halliday, G.M., 2016. The substantia nigra and ventral tegmental dopaminergic neurons from development to degeneration. J Chem Neuroanat. 76 (Pt B), 98–107. https://doi.org/10.1016/j.jchemneu.2016.02.001.

Gaser, C., Dahnke, R., 2016. CAT – A Computational Anatomy Toolbox for the Analysis of Structural MRI Data. OHBM Annual Meeting. 336–348.

Glasser, M.F., Coalson, T.S., Robinson, E.C., Hacker, C.D., Harwell, J., Yacoub, E., Ugurbil, K., Andersson, J., Beckmann, C.F., Jenkinson, M., Smith, S.M., Van Essen, D. C., 2016. A multi-modal parcellation of human cerebral cortex. Nature. 536 (7615), 171–178. https://doi.org/10.1038/nature18933.

Haber, S.N., 2014. The place of dopamine in the cortico-basal ganglia circuit. Neuroscience. 282, 248–257. https://doi.org/10.1016/j.neuroscience.2014.10.008.

Harada, C.N., Natelson Love, M.C., Triebel, K.L., 2013. Normal cognitive aging. Clin Geriatr Med. 29 (4), 737–752. https://doi.org/10.1016/j.cger.2013.07.002.

Hedden, T., Gabrieli, J.D., 2004. Insights into the ageing mind: a view from cognitive neuroscience. Nat Rev Neurosci. 5 (2), 87–96. https://doi.org/10.1038/nrn1323.

Heinrichs-Graham, E., Santamaria, P.M., Gendelman, H.E., Wilson, T.W., 2017. The cortical signature of symptom laterality in Parkinson's disease. Neuroimage Clin. 12 (14), 433–440. https://doi.org/10.1016/j.nicl.2017.02.010.

Hu, S., Ide, J.S., Chao, H.H., Castagna, B., Fischer, K.A., Zhang, S., Li, C.R., 2018. Structural and functional cerebral bases of diminished inhibitory control during healthy aging. Hum Brain Mapp. 39 (12), 5085–5096. https://doi.org/10.1002/hbm.24347.

Jacobs, H.I.L., Wiese, S., van de Ven, V., Gronenschild, E.H., Verhey, F.R., Matthews, P. M., 2015. Relevance of parahippocampal-locus coeruleus connectivity to memory in early dementia. Neurobiol Aging. 36 (2), 618–626. https://doi.org/10.1016/j.neurobiolaging.2014.10.041.

Jacobs, H.I.L., Müller-Ehrenberg, L., Priovoulos, N., Roebroeck, A., 2018. Curvilinear locus coeruleus functional connectivity trajectories over the adult lifespan: a 7T MRI study. Neurobiol Aging. 69, 167–176. https://doi.org/10.1016/j.neurobiolaging.2018.05.021.

Jenkinson, M., Beckmann, C.F., Behrens, T.E.J., Woolrich, M.W., Smith, S.M., 2012. FSL. FSL. Neuroimage. 62 (2), 782–790.

Jockwitz, C., Caspers, S., 2021. Resting-state networks in the course of aging-differential insights from studies across the lifespan vs. amongst the old. Pflugers Arch. 473 (5), 793–803. https://doi.org/10.1007/s00424-021-02520-7.

Karim, H.T., Rosso, A., Aizenstein, H.J., Bohnen, N.I., Studenski, S., Rosano, C., 2020. Resting state connectivity within the basal ganglia and gait speed in older adults with cerebral small vessel disease and locomotor risk factors. Neuroimage Clin. 28, 102401 https://doi.org/10.1016/j.nicl.2020.102401.

Karrer, T.M., Josef, A.K., Mata, R., Morris, E.D., Samanez-Larkin, G.R., 2017. Reduced dopamine receptors and transporters but not synthesis capacity in normal aging adults: a meta-analysis. Neurobiol Aging. 57, 36–46. https://doi.org/10.1016/j.neurobiolaging.2017.05.006.

Kloke J, McKean J. Nonparametric Statistical Methods Using R. 2000. London, the United Kingdom: Chapman and Hall/CRC.

Kriegeskorte, N., Lindquist, M.A., Nichols, T.E., Poldrack, R.A., Vul, E., 2010. Everything you never wanted to know about circular analysis, but were afraid to ask. J Cereb Blood Flow Metab. 30 (9), 1551–1557. https://doi.org/10.1038/jcbfm.2010.86.

Liebe, T., Kaufmann, J., Li, M., Skalej, M., Wagner, G., Walter, M., 2020. In vivo anatomical mapping of human locus coeruleus functional connectivity at 3 T MRI. Hum Brain Mapp. 41 (8), 2136–2151. https://doi.org/10.1002/hbm.24935.

Madan, C.R., 2018. Age differences in head motion and estimates of cortical morphology. PeerJ. 6 (e5176) https://doi.org/10.7717/peerj.5176.

Manza, P., Zhang, S., Hu, S., Chao, H.H., Leung, H.C., Li, C.R., 2015. The effects of age on resting state functional connectivity of the basal ganglia from young to middle adulthood. Neuroimage. 107, 311–322. https://doi.org/10.1016/j.neuroimage.2014.12.016.

Meola, A., Comert, A., Yeh, F.C., Sivakanthan, S., Fernandez-Miranda, J.C., 2016. The nondecussating pathway of the dentatorubrothalamic tract in humans: human

connectome-based tractographic study and microdissection validation. J Neurosurg. 124 (5), 1406–1412. https://doi.org/10.3171/2015.4.JNS142741.
Minassian, A., Young, J.W., Cope, Z.A., Henry, B.L., Geyer, M.A., Perry, W., 2016. Amphetamine increases activity but not exploration in humans and mice. Psychopharmacology (Berl). 233 (2), 225–233. https://doi.org/10.1007/s00213-015-4098-4.
Mitchell, A.S., Chakraborty, S., 2013. What does the mediodorsal thalamus do? Front Syst Neurosci. 7, 37. https://doi.org/10.3389/fnsys.2013.00037.
Molochnikov, I., Cohen, D., 2014. Hemispheric differences in the mesostriatal dopaminergic system. Front Syst Neurosci. 8, 110. https://doi.org/10.3389/fnsys.2014.00110.
Murty, V.P., Shermohammed, M., Smith, D.V., Carter, R.M., Huettel, S.A., Adcock, R.A., 2014. Resting state networks distinguish human ventral tegmental area from substantia nigra. Neuroimage. 100, 580–589. https://doi.org/10.1016/j.neuroimage.2014.06.047.
Pauli, W.M., Nili, A.N., Tyszka, J.M., 2018. A high-resolution probabilistic in vivo atlas of human subcortical brain nuclei. Sci Data. 5, 180063 https://doi.org/10.1038/sdata.2018.63.
Peterson, A.C., Li, C.R., 2018. Noradrenergic Dysfunction in Alzheimer's and Parkinson's Diseases-An Overview of Imaging Studies. Front Aging Neurosci. 1 (10), 127. https://doi.org/10.3389/fnagi.2018.00127.
Peterson, A.C., Zhang, S., Hu, S., Chao, H.H., Li, C.R., 2017. The Effects of Age, from Young to Middle Adulthood, and Gender on Resting State Functional Connectivity of the Dopaminergic Midbrain. Front Hum Neurosci. 11, 52. https://doi.org/10.3389/fnhum.2017.00052.
R Core Team. R: A language and environment for statistical computing. 2021. Vienna, Austria: R Foundation for Statistical Computing.
Rademacher, L., Salama, A., Gründer, G., Spreckelmeyer, K.N., 2014. Differential patterns of nucleus accumbens activation during anticipation of monetary and social reward in young and older adults. Soc Cogn Affect Neurosci. 9 (6), 825–831. https://doi.org/10.1093/scan/nst047.
Ramos, B.P., Arnsten, A.F., 2007. Adrenergic pharmacology and cognition: focus on the prefrontal cortex. Pharmacol Ther. 113 (3), 523–536. https://doi.org/10.1016/j.pharmthera.2006.11.006.
Reitan, R.M., Wolfson, D., 2004. The Trail Making Test as an initial screening procedure for neuropsychological impairment in older children. Arch Clin Neuropsychol. 19 (2), 281–288. https://doi.org/10.1016/S0887-6177(03)00042-8.
Saloner, R., Cherner, M., Sundermann, E.E., Watson, C.W., Iudicello, J.E., Letendre, S.L., Kumar, A., Ellis, R.J., 2020. COMT val158met genotype alters the effects of methamphetamine dependence on dopamine and dopamine-related executive function: preliminary findings. Psychiatry Res. 292, 113269 https://doi.org/10.1016/j.psychres.2020.113269.
Schultz, W., 2016. Dopamine reward prediction error coding. Dialogues Clin Neurosci. 18 (1), 23–32. https://doi.org/10.31887/DCNS.2016.18.1/wschultz.
Song, I., Neal, J., Lee, T.H., 2021. Age-Related Intrinsic Functional Connectivity Changes of Locus Coeruleus from Childhood to Older Adults. Brain Sci. 11 (11), 1485. https://doi.org/10.3390/brainsci11111485.
Song, X., Zhang, Y.i., Liu, Y., Lin, F.-H., 2014. Frequency specificity of regional homogeneity in the resting-state human brain. PLoS One. 9 (1) https://doi.org/10.1371/journal.pone.0086818.
St-Hilaire, A., Parent, C., Potvin, O., Bherer, L., Gagnon, J.F., Joubert, S., Belleville, S., Wilson, M.A., Koski, L., Rouleau, I., Hudon, C., Macoir, J., 2018. Trail Making Tests A and B: regression-based normative data for Quebec French-speaking mid and older aged adults. Clin Neuropsychol. 32 (sup1), 77–90. https://doi.org/10.1080/13854046.2018.1470675.
Swirsky, L.T., Spaniol, J., 2019. Cognitive and motivational selectivity in healthy aging. Wiley Interdiscip Rev Cogn Sci. 10 (6), e1512.
Szabadi, E., 2013. Functional neuroanatomy of the central noradrenergic system. J Psychopharmacol. 27 (8), 659–693. https://doi.org/10.1177/0269881113490326. Erratum. In: J Psychopharmacol. 2013; 27(10):964.
Tsvetanov, K.A., Henson, R.N.A., Rowe, J.B., 2021. Separating vascular and neuronal effects of age on fMRI BOLD signals. Philos Trans R Soc Lond B Biol Sci. 376 (1815), 20190631. https://doi.org/10.1098/rstb.2019.0631.
Vallesi, A., Tronelli, V., Lomi, F., Pezzetta, R., 2021. Age differences in sustained attention tasks: A meta-analysis. Psychon Bull Rev. 28 (6), 1755–1775.
Yarkoni, T., Poldrack, R.A., Nichols, T.E., Van Essen, D.C., Wager, T.D., 2011. Large-scale automated synthesis of human functional neuroimaging data. Nat Methods. 8 (8), 665–670. https://doi.org/10.1038/nmeth.1635.
Zang, Y., Jiang, T., Lu, Y., He, Y., Tian, L., 2004. Regional homogeneity approach to fMRI data analysis. Neuroimage. 22 (1), 394–400. https://doi.org/10.1016/j.neuroimage.2003.12.030.
Zhang, S., Hu, S., Chao, H.H., Li, C.S., 2016. Resting-State Functional Connectivity of the Locus Coeruleus in Humans. In Comparison with the Ventral Tegmental Area/Substantia Nigra Pars Compacta and the Effects of Age. Cereb Cortex. 26 (8), 3413–3427. https://doi.org/10.1093/cercor/bhv172.
Zhang, Y., Larcher, K.M., Misic, B., Dagher, A., 2017. Anatomical and functional organization of the human substantia nigra and its connections. Elife. 6, e26653.
Zimmermann P, Fimm B. Testbatterie zur Aufmerksamkeitsprüfung Version 2.3. 2012. Psychologische Testsysteme.